

Enhanced stress-invariance of magnetization direction in magnetic thin films

Xinyu Qiao,^{1,2,3,a)} Xingcheng Wen,^{1,2,4,a)} Baomin Wang,^{1,2,b)} Yuhao Bai,³ Qingfeng Zhan,^{1,2} Xiaohong Xu,^{3,b)} and Run-Wei Li^{1,2,b)}

¹CAS Key Laboratory of Magnetic Materials and Devices, Ningbo Institute of Materials Technology and Engineering, Chinese Academy of Sciences, Ningbo 315201, People's Republic of China

²Zhejiang Province Key Laboratory of Magnetic Materials and Application Technology, Ningbo Institute of Materials Technology and Engineering, Chinese Academy of Sciences, Ningbo 315201, People's Republic of China

³Key Laboratory of Magnetic Molecules and Magnetic Information Materials of Ministry of Education, School of Chemistry and Materials Science, Shanxi Normal University, Linfen 041004, People's Republic of China

⁴Institute of Materials Science, School of Materials Science and Engineering, Shanghai University, Shanghai 200072, People's Republic of China

(Received 15 June 2017; accepted 17 September 2017; published online 26 September 2017)

Spin valve devices, consisting of a free magnetic layer, a spacer layer, and a pinned magnetic layer, are widely used in magnetic sensors and nonvolatile magnetic memories. However, even a slight bending deformation can affect the magnetization direction of the free magnetic layer, which will change the magnetoresistance signal of the devices. Therefore, it is a challenge to develop a flexible spin valve device with controllable performance. Here, an enhanced stress-invariance of the magnetization direction in amorphous CoFeB magnetic films on flexible polyimide substrates is achieved. The uniaxial anisotropy is induced by growing on the bent substrate under a magnetic field, which aligns more magnetic domains with easy axes along the direction perpendicular to the subsequently applied stress. Theoretical calculations indicate that pre-induced anisotropy with an easy axis perpendicular to the applied stress effectively resists the change in the magnetization direction during bending. These results are of importance for realizing better performance of flexible spin valve devices and the development of flexible spintronics. *Published by AIP Publishing.* [<http://dx.doi.org/10.1063/1.4990571>]

Flexible electronics has emerged as one of the most rapidly developing technologies owing to the advantages in processing cost and mechanical stretchability over conventional silicon-based counterparts.^{1,2} It has driven the developments of many devices such as flexible transistors,³ capacitors,⁴ implantable medical devices,⁵ and even magnetoresistive sensors.^{6–9} Spin valve (SV) devices, consisting of a free magnetic layer, a spacer layer, and a pinned magnetic layer, are broadly applied in magnetic sensors and nonvolatile magnetic memories.¹⁰ They are based on the giant magnetoresistance (GMR) effect or the tunneling magnetoresistance (TMR) effect,^{11,12} which are dependent on the relative magnetization direction between the free and pinned magnetic layers. CoFeB films have been used widely as the sensing layers in TMR based SV devices because of their high spin polarization.^{13,14} However, the magnetic anisotropy of CoFeB can be changed by applied stress on the flexible substrates due to inverse magnetostrictive effects and magnetoelastic coupling effects,^{15,16} resulting in changes in the magnetoresistance signal of the SV devices. For example, Fig. 1(a) shows the magnetization directions of the free and pinned magnetic layers in the low resistance state of a SV. The magnetization of the free layer will rotate during bending due to the stress-induced change in the easy axis of magnetic anisotropy^{15,16} [Fig. 1(b)]. Increasing the bending beyond the limit of the antiferromagnetic pinning effect will change the magnetization direction of

the pinned layer, as shown in Fig. 1(c). Since the magnetic anisotropy of the free layer is uniaxial, its magnetic moments may not return to the original direction after the bending [Fig. 1(d)]. As a result, the original low resistance state will be destroyed. It is very important to develop a method to prepare the magnetic films, so as to make their magnetic easy axis insensitive to the applied stress during bending.

In this work, we design a method to fabricate flexible magnetic films by dc magnetron sputtering as shown in Fig. 2(a). A magnetic field is applied perpendicular to the bending direction during deposition. After deposition, the film is released from the convex mold, flattened to a plane [Fig. 2(b)], and subjected to a compressive strain due to the rigid clamping at the substrate interface.^{17,18} Both substrate bending and applied magnetic field are used to enhance the anisotropy of magnetic layers in the present work.^{17–19} The easy axis of prepared CoFeB films in various states is shown in Figs. 2(c)–2(e). Figure 2(f) schematically represents the magnitude of the magnetic anisotropy from magnetic-field-induced and stress-induced anisotropy in different states. The magnetic anisotropy induced by stress will decrease (increase) under tensile (compressive) strain,¹⁵ while that induced by the magnetic field is nearly constant. Thus, the easy axis of the film is unchanged under various strains, that is, the magnetization direction of films is insensitive to subsequently applied stress and can be used for flexible SV devices. We test this promise in what follows.

70 nm thick amorphous CoFeB films were fabricated on Polyimide (PI) substrates at room temperature by dc magnetron sputtering.^{15,16} The base pressure of the sputtering

^{a)}X. Qiao and X. Wen contributed equally to this work.

^{b)}Authors to whom correspondence should be addressed: wangbaomin@nimte.ac.cn; xuxiaohong_ly@163.com; and runweili@nimte.ac.cn.

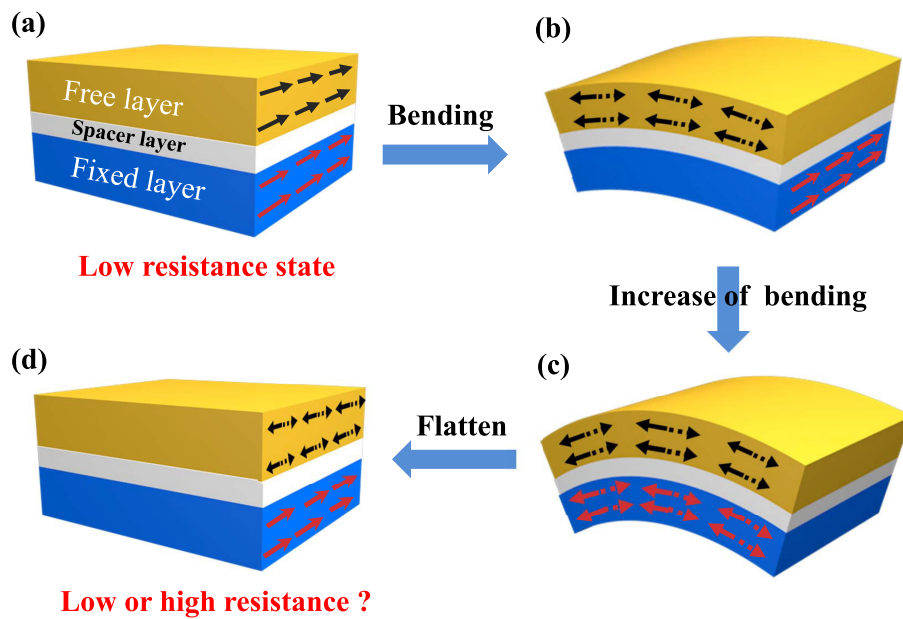


FIG. 1. (a) The simple diagram of the ideal spin valve sketch. (b) and (c) The change in magnetization directions of the free magnetic layer and pinned magnetic layer during bending. (d) The magnetization directions of the free magnetic layer and pinned magnetic layer after releasing from bending.

chamber is better than 1.0×10^{-7} Torr. Before being placed into the sputtering chamber, the PI substrates were cleaned ultrasonically in ethanol for 15 min and then dried with nitrogen gas. The substrates were fixed on molds using double-sided tape with certain curvatures represented by the mold radii. A couple of permanent magnets placed on both sides of the mold provided a uniform magnetic field of 1200 Oe during the film deposition to induce an extra magnetic anisotropy, as schematically illustrated in Fig. 2(a). During deposition, the Ar flow was kept at 39 sccm and the pressure was set at 4.0×10^{-3} Torr. The deposition power was kept at 50 W. The deposition rate was 1.2 nm/min. Prior to be taken out from the chamber, a 3 nm Ta layer was deposited on the CoFeB films to prevent oxidation. The angular dependent

hysteresis loops under different tensile and compressive strains generated via outward and inward bending of the simple were measured using a vibrating sample magnetometer (VSM, Lakeshore 7410) at room temperature. The film thickness was measured using a surface profilometer (KLA Tencor, Alpha-Step IQ).

Figure 3(a) shows the magnetic hysteresis loops of a CoFeB film on a flexible PI substrate. The film was released from the convex molds and flattened and measured with magnetic fields along x and y directions, respectively. It is clear that the film has an in-plane magnetic anisotropy. Figure 3(b) shows the angular dependence of normalized remanent magnetization (M_r/M_s), which oscillates with 180° periodicity, showing a uniaxial anisotropy in the CoFeB

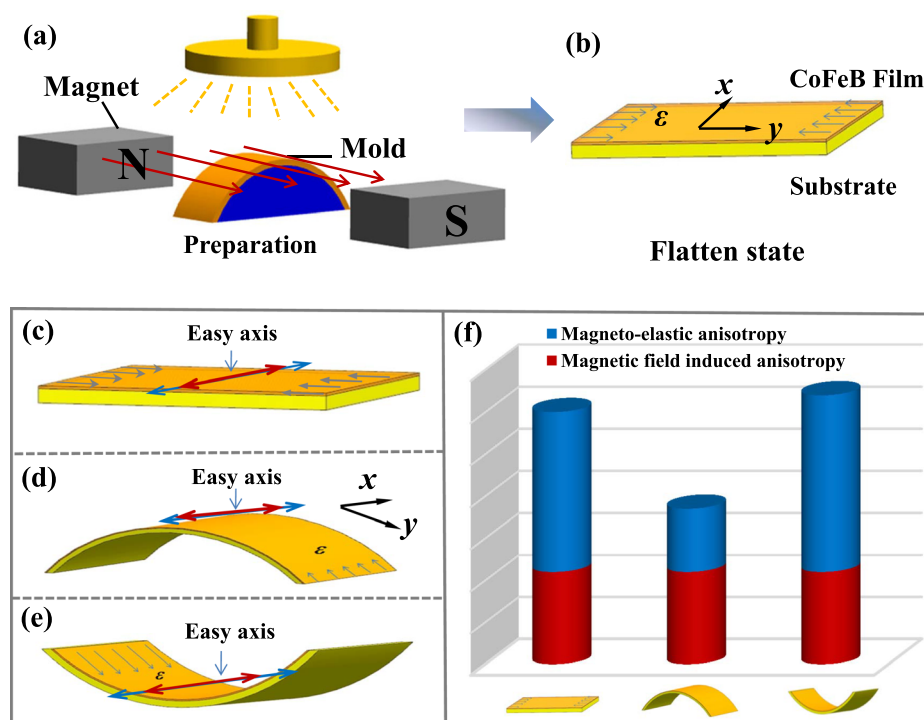


FIG. 2. (a) An illustrative drawing of the experimental setup for sample fabrication during the depositing process, and both bowed growth and magnetic field are used to induce the anisotropy of magnetic materials. (b) Diagram of the flatten state of the magnetic film after deposition. A compressive stress is produced in the film when the substrate is shaped from convex to flat. The illustrative drawing of different bending states of the magnetic film: (c) flatten state and (d) convex and (e) concave molds. The red arrow represents an easy axis induced by stress, and the blue arrow represents an easy axis induced by the applied field. (f) Schematic drawing of the magnitude of magnetic anisotropy contributed from two terms (magnetic-field-induced and stress-induced anisotropy) in different strain states, which corresponds to Figs. 2(c)–2(e).

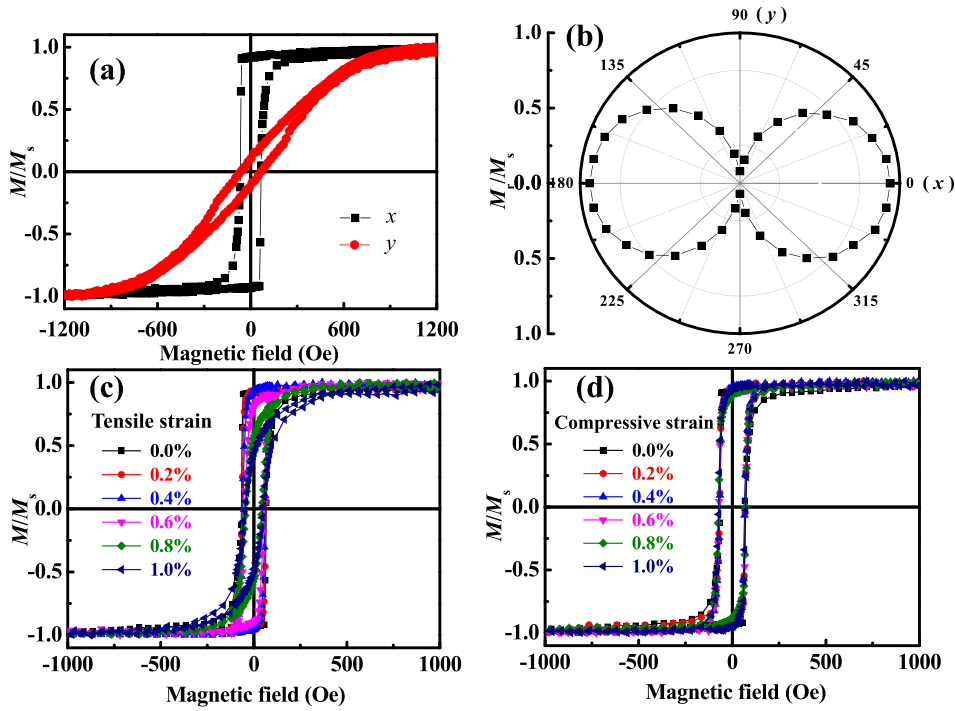


FIG. 3. (a) Hysteresis loops of 70 nm CoFeB along x and y directions. (b) Angular dependence of normalized M_t/M_s of the 70 nm CoFeB film. (c) and (d) Hysteresis loops of the 70 nm CoFeB films in different strain states: (c) tensile strains and (d) compressive strains.

film. It shows that the easy axis is along the x direction and the hard axis along the y direction. In order to study the stress dependent magnetic anisotropy, we designed several molds with different radii to apply various tensile or compressive strains. Figures 3(c) and 3(d) show the hysteresis loops of the CoFeB films under various strains, in which the flexible substrates are bent along the hard axis (y direction). For all the magnetization measurements, the applied magnetic field is in the plane of the film and perpendicular to the bending direction to make sure that the measured signals are from in-plane magnetic moments. When the sample is subjected to tensile strain, the square hysteresis loop is changed to a slanted one, and the M_t/M_s decreases from 0.92 to 0.43 with the increasing tensile strain. On the contrary, the shape of the hysteresis loop remains unchanged, and M_t/M_s is almost constant when the sample is under compressive strain.

For comparative analysis, a CoFeB thin film prepared on a flexible substrate without any external factors to induce magnetic anisotropy was also subjected to bending tests. The M_t/M_s values of samples prepared in different strain states are

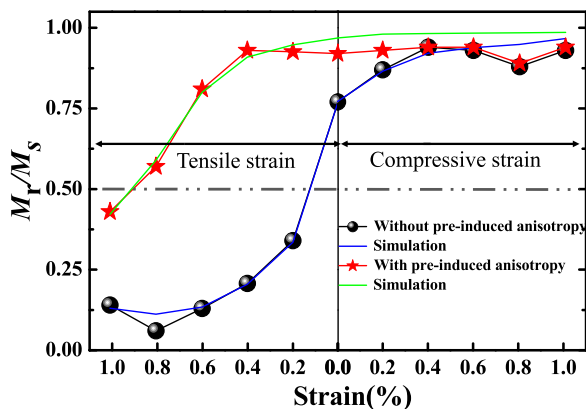


FIG. 4. The strain dependence of normalized M_t/M_s for bending CoFeB films with and without pre-induced magnetic anisotropy, respectively.

summarized in Fig. 4. It shows that the normalized M_t/M_s of the film prepared without pre-induced magnetic anisotropy changes sharply from 0.77 to 0.14 under subsequent tensile strain. In contrast, M_t/M_s along the easy axis only changes from 0.92 to 0.43 for the film with pre-induced magnetic anisotropy, that is, the magnetic easy axis is more resistant to a change in the film with pre-induced magnetic anisotropy.

To gain further insights into the enhanced stress-invariance of the magnetization direction when extra magnetic anisotropy is induced during deposition, theoretical analysis is conducted. We perform simulations based on the modified Stoner-Wohlfarth model.²⁰ The total free energy E of the amorphous CoFeB film we designed can be written as $E = K_U \sin^2\theta + K_\sigma \sin^2(\varphi - \theta) - HM \cos(\theta_H - \theta)$, where K_U is the initial uniaxial magnetic anisotropy (the magnetic anisotropy in the flatten state), K_σ is the uniaxial magnetic anisotropy induced by applied stress, and φ is the angle between the easy axes of the initial anisotropy and that induced by the applied stress. θ and θ_H are the angles between the magnetization and the measured magnetic field with the easy axis of the initial uniaxial anisotropy K_U , respectively. The uniaxial magnetic anisotropy induced by stress can be calculated by $K_\sigma = -3\varepsilon\lambda_s E_f / 2(1 - \nu^2)$, where E_f is the Young's modulus of the CoFeB film (~ 162 GPa),²¹ ν is the Poisson ratio of the CoFeB film (~ 0.3),²² λ_s is the magnetostriction constant of the amorphous CoFeB film (~ 35 ppm),²¹ and ε is the applied strain. The applied strain can be calculated by $\varepsilon = (h + t)/(2r + h + t)$, h is the thickness of the film, t is the thickness of the substrate, and r is the bending radius. For the CoFeB film deposited with substrate bending and magnetic field, the M_t/M_s of the hysteresis loop is less (more) than one (zero) along the easy (hard) axis [Fig. 3(a)], which indicates that the easy axes of CoFeB magnetic domains do not strictly orient in one direction but have a distribution along its average direction [Fig. 5(a)]. The easy axis of each domain will be modulated by the applied

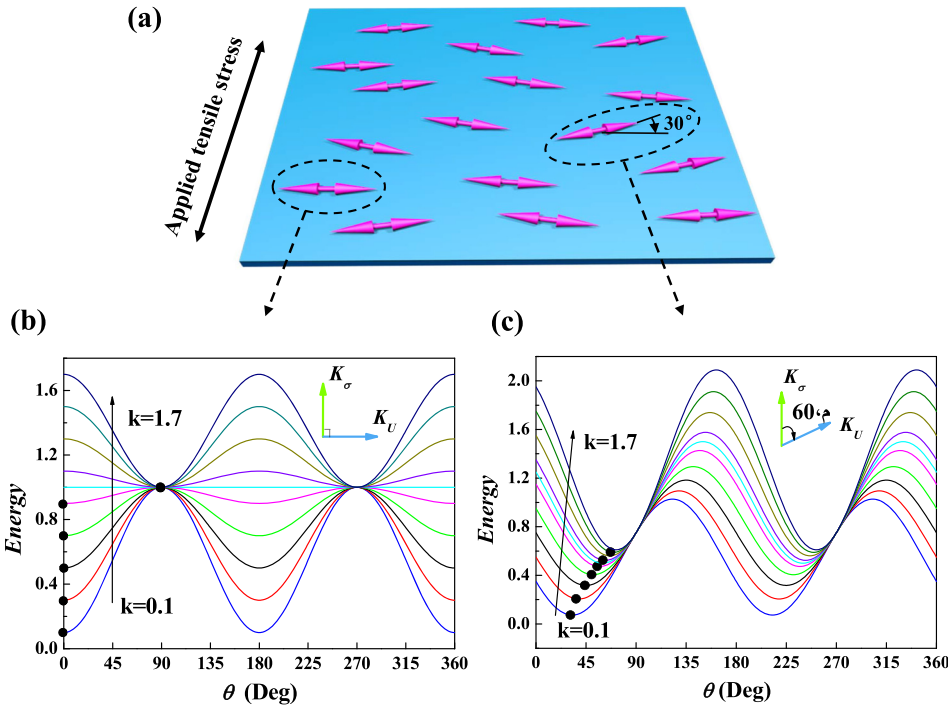


FIG. 5. Schematic diagram of the theoretical system. (a) The system is composed of magnetic domains with effective uniaxial magnetic anisotropy (double arrow). (b) and (c) The corresponding angular dependence of the energy for the magnetic film when the stress is applied perpendicular and with 30° to the easy direction of the effective uniaxial magnetic anisotropy. k increases from 0.1 to 1.7 with an interval of 0.2. The stable positions of M have been indicated by the black solid circles.

stress, which can be expressed by the normalized stress induced anisotropy k defined as $k = K_\sigma / K_U$. For example, considering a magnetic domain with its easy axis of the uniaxial anisotropy, K_U , perpendicular to the easy axis of the stress-induced anisotropy, K_σ ($\varphi = 90^\circ$), if a smaller stress is applied, its energy will increase, but the magnetization orientation remains the same, as shown in Fig. 5(b). A sudden change in the magnetization direction will appear when k is beyond a critical value, along with the change in the magnetization direction. If the angle between the applied stress and the easy axis of K_U is less than 90° , such as $\varphi = 60^\circ$, the easy axis will gradually shift with increasing stress, and no critical value of k will be exhibited, i.e., the magnetization varies continuously [Fig. 5(c)]. Based on these results, we simulated the M_r/M_s of films prepared with and without pre-induced magnetic anisotropy in different strain states, considering that the easy axis of the magnetic domains follow a distribution function of $f(\varphi) = \cos^n(\varphi - \Psi)$.²⁰ Here, Ψ stands for the average easy axes of all the magnetic domains, and n is the factor describing the dispersion of the easy axis distribution. In general, for a given value of Ψ , a larger n will give a narrower distribution of the easy axis. When the stress is gradually increased, n will increase gradually and Ψ is close to 0° (i.e., the positive x axis), which means that more and more magnetic domains rotate their easy axes to the direction of the stress-induced anisotropy. By adjusting the values of Ψ and n according to the stress, M_r/M_s can be calculated by the following formula: $\frac{M_r}{M_s} = \frac{\int_0^{\pi/2} \cos(\varphi) f(\varphi) \sin \varphi d\varphi}{\int_0^{\pi/2} f(\varphi) \sin \varphi d\varphi}$.²⁰ We found that the behavior of the calculated M_r/M_s is basically identical to the experimental results, as shown in Fig. 4. Therefore, magnetic films prepared with substrate bending and magnetic field contain more magnetic domains with easy axes along the direction perpendicular to the subsequently applied tensile stress. As a

result, they can effectively resist the change in the magnetization direction under applied stress subsequently.

In summary, we have designed a method to fabricate amorphous CoFeB films on flexible substrates by magnetron sputtering, in which the substrates are fixed on convex molds, and a magnetic field is applied during the film growth. Both the applied stress and magnetic field induce magnetic anisotropy in the thin films. The M_r/M_s of the resulting thin films changes more slowly than that of the films without a pre-induced magnetic anisotropy under subsequent bending tests. Our study suggests that the film we designed can bear the applied stress within the bending radius of deposition without degradation of the key properties of SV devices. These results are of importance for better performance of flexible SV devices.

We would like to thank Professor Junling Wang for fruitful discussions. This work was supported by the National Key R&D Program of China (2016YFA0201102), the National Natural Science Foundation of China (51571208, 51301191, 51525103, 11404202, 11474295, and 51401230), the Youth Innovation Promotion Association of the Chinese Academy of Sciences (2016270), the Key Research Program of the Chinese Academy of Sciences (KJZD-EW-M05), the Ningbo Major Project for Science and Technology (2014B11011), the Ningbo Science and Technology Innovation Team (2015B11001), and the Ningbo Natural Science Foundation (2015A610110).

¹D.-H. Kim and J. A. Rogers, *Adv. Mater.* **20**, 4887 (2008).

²R. L. Crabb and F. C. Treble, *Nature* **213**, 1223 (1967).

³H.-C. Yuan and Z. Q. Ma, *Appl. Phys. Lett.* **89**, 212105 (2006).

⁴J. Rho, S. J. Kim, W. Heo, N.-E. Lee, H.-S. Lee, and J.-H. Ahn, *IEEE Electron Device Lett.* **31**, 1017 (2010).

⁵J. Viventi, D.-H. Kim, J. D. Moss, Y.-S. Kim, J. A. Blanco, N. Annetta, A. Hicks, J. Xiao, Y. Huang, D. J. Callans, J. A. Rogers, and B. Litt, *Sci. Transl. Med.* **2**, 24ra22 (2010).

- ⁶C. Barraud, C. Deranlot, P. Seneor, R. Mattana, B. Dlubak, S. Fusil, K. Bouzehouane, D. Deneuue, F. Petroff, and A. Fert, *Appl. Phys. Lett.* **96**, 072502 (2010).
- ⁷M. Melzer, D. Makarov, A. Calvimontes, D. Karnaushenko, S. Baunack, R. Kaltofen, Y. F. Mei, and O. G. Schmidt, *Nano Lett.* **11**, 2522 (2011).
- ⁸A. Bedoya-Pinto, M. Donolato, M. Gobbi, L. E. Hueso, and P. Vavassori, *Appl. Phys. Lett.* **104**, 062412 (2014).
- ⁹M. Melzer, G. Lin, D. Makarov, and O. G. Schmidt, *Adv. Mater.* **24**, 6468–6472 (2012).
- ¹⁰G. A. Prinz, *Science* **282**, 1660 (1998).
- ¹¹M. N. Baibich, J. M. Broto, A. Fert, F. Nguyen Van Dau, F. Petroff, P. Etienne, G. Creuzet, A. Friederich, and J. Chazelas, *Phys. Rev. Lett.* **61**, 2472 (1988).
- ¹²G. Binasch, P. Grünberg, F. Saurenbach, and W. Zinn, *Phys. Rev. B* **39**, 4828 (1989).
- ¹³S. S. Parkin, C. Kaiser, A. Panchula, P. M. Rice, B. Hughes, M. Samant, and S. H. Yang, *Nat. Mater.* **3**, 862 (2004).
- ¹⁴S. Ikeda, K. Miura, H. Yamamoto, K. Mizunuma, H. D. Gan, M. Endo, S. Kanai, J. Hayakawa, F. Matsukura, and H. Ohno, *Nat. Mater.* **9**, 721 (2010).
- ¹⁵Z. H. Tang, B. M. Wang, H. L. Yang, X. Y. Xu, Y. W. Liu, D. D. Sun, L. X. Xia, Q. F. Zhan, B. Chen, M. H. Tang, Y. C. Zhou, J. L. Wang, and R. W. Li, *Appl. Phys. Lett.* **105**, 103504 (2014).
- ¹⁶Y. W. Liu, B. M. Wang, Q. F. Zhan, Z. H. Tang, H. L. Yang, G. Liu, Z. H. Zuo, X. S. Zhang, Y. L. Xie, X. J. Zhu, B. Chen, J. L. Wang, and R. W. Li, *Sci. Rep.* **4**, 6615 (2014).
- ¹⁷X. Y. Qiao, B. M. Wang, Z. H. Tang, Y. Shen, H. L. Yang, J. L. Wang, Q. F. Zhan, S. N. Mao, X. H. Xu, and R. W. Li, *AIP Adv.* **6**, 056106 (2016).
- ¹⁸Y. Yu, Q. F. Zhan, J. W. Wei, J. B. Wang, G. H. Dai, Z. H. Zuo, X. S. Zhang, Y. W. Liu, H. L. Yang, Y. Zhang, S. H. Xie, B. M. Wang, and R. W. Li, *Appl. Phys. Lett.* **106**, 162405 (2015).
- ¹⁹A. T. Hindmarch, D. A. Arena, K. J. Dempsey, M. Henini, and C. H. Marrows, *Phys. Rev. B* **81**, 100407 (2010).
- ²⁰T. M. L. Alves, C. G. Bezerra, A. D. C. Viegas, S. Nicolodi, M. A. Correa, and F. Bohn, *J. Appl. Phys.* **117**, 083901 (2015).
- ²¹A. T. Hindmarch, A. W. Rushforth, R. P. Champion, C. H. Marrows, and B. L. Gallagher, *Phys. Rev. B* **83**, 212404 (2011).
- ²²N. Lei, S. Park, P. Lecoeur, D. Ravelosona, C. Chappert, O. Stelmakhovych, and V. Holy, *Phys. Rev. B* **84**, 012404 (2011).